

O/SO Gauge Groups, BC Quivers and $O3$ Planes

Sam Bennett , Amihay Hanany

*Abdus Salam Centre for Theoretical Physics, Imperial College London,
Prince Consort Road London, SW7 2AZ, UK*

E-mail: samuel.bennett18@imperial.ac.uk, a.hanany@imperial.ac.uk

ABSTRACT: D3-/D5-/NS5-brane systems with $O3$ orientifold planes realise 3d $\mathcal{N} = 4$ gauge theories with orthogonal and symplectic gauge groups on the D3-brane worldvolume. Such setups have long contained an ambiguity regarding the global form of D -type gauge groups. This note offers a partial prescription for reading $O(2k)$ and $SO(2k)$ gauge nodes in orthosymplectic quivers using the presence of $\frac{1}{2}$ D5-branes on the orientifolds bordering $\frac{1}{2}$ NS5-brane intervals spanned by $O3^-$ planes. A set of identities are proposed relating the Coulomb branches of generic quivers under a Higgsing that relates $SO(2k + 1)$ and $O(2k)$ gauge groups. A further prescription is conjectured regarding the action of $\frac{1}{2}$ D5-branes on maximal DC -chains.

Contents

1	Introduction	1
2	Brane and Quiver Conventions	3
2.1	Quiver Derivation Rules	3
2.2	$O(2n)$ versus $SO(2n)$	5
3	A Motivating Example: $O(3)$ with N_f Flavours	8
4	The $B_n \leftrightarrow O(2n)$ Identity	10
4.1	As a Higgsing	11
4.2	Special Piece Generalisation	13
5	The BC- and CB-Chains	13
6	Gauging \mathbb{Z}_2 Flavour Subgroups of $Sp(k)$ SQCD	14
6.1	Example	17
7	Outlook	19
A	Evidence for Identities	19
B	Hilbert Series for BC Chains	23

1 Introduction

An interesting feature of the recent history of unitary quiver gauge theories with eight supercharges is the extent to which a surprisingly general set of algorithms captures the essential data of the moduli space [1–12]. This builds upon the simple fact that the moduli space of a 3d $\mathcal{N} = 4$ gauge theory is a symplectic singularity in the sense of Beauville [13], and as such admits a symplectic stratification into so-called ‘minimal degenerations’ whose partial order can be captured using a Hasse¹ diagram [14–17]. In 3d $\mathcal{N} = 4$ theories, scalar fields in the hypermultiplets and vectormultiplets partition the total moduli space into two hyper-Kähler spaces known as the Higgs and Coulomb branches, parametrised by the VEVs of each set of scalars respectively. Although the Higgs branch is classically exact on account of the nonrenormalisation theorem, the Coulomb branch is corrected in the quantum theory through the contributions of monopole operators [18, 19], parametrised by the Weyl orbits of the weight lattice of the Langlands dual of the gauge group. Despite these complexities, the rigid symplectic holomorphic structure imposed by the supersymmetry encodes the symplectic stratification of the Coulomb and Higgs branches into the quivers themselves — the quiver subtraction programme has over the past few years developed several methods for the calculation of Hasse diagrams from quiver combinatorics.

¹Symplectic singularity structure emerges from the supersymmetry — the moduli space of a 3d $\mathcal{N} = 2$ theory is often a Gorenstein singularity, whose stratification is far less studied.

Although Higgs branch quiver subtraction [11] can be derived purely from the classical Higgs mechanism (or equivalently by interpreting the Higgs branch as the hyper-Kähler quotient of the moduli space of representations of the quiver ²), quantum corrections on the Coulomb branch require further information, such as from a brane system, in order to capture the full picture; for unitary simply-laced quivers, such is provided using configurations of D3-branes, D5-branes and NS5-branes in the tradition of Hanany-Witten [20]. The inclusion of orientifold planes in D3-/D5-/NS5-brane systems [21, 22], which results in orthosymplectic and non-simply laced 3d $\mathcal{N} = 4$ quivers arising as low-energy worldvolume theories on the D3-branes [22, 23], complicates the analysis significantly. Roughly, the orientifold planes move the natural reference point for the moduli spaces of such theories from the nilpotent cone of \mathfrak{sl}_n to those of the classical algebras of types $B/C/D$, introducing new features such as non-normality, non-special orbits and the canonical quotient of Lusztig [24–26].

One of the most fundamental obstacles to realising an algorithm for Coulomb branch quiver subtraction on framed orthosymplectic quivers is the problem of determining the global form of the gauge group. The Chan-Paton prescription [27] specifies the gauge group of the resulting theory on a stack of D-branes in the presence of an orientifold, favouring $O(n)$ rather than $SO(n)$ gauge groups. In quiver gauge theory, a lack of tools for dealing with discrete groups leaves an ambiguity between $SO(2N)$ and $O(2N)$ gauge theories in NS5-brane intervals spanned by $O3^-$ planes. Recent work [28] on framed orthosymplectic quivers using the framework of nilpotent cones has emphasised the importance of $SO(2N)$ versus $O(2N)$ — gauging an extra \mathbb{Z}_2 in general changes the Coulomb branch (its effect on the Higgs branch was considered in [29–31]).

This note conjectures a rule for reading individual $O(2n)$ and $SO(2n)$ gauge nodes from D3/D5/NS5-brane systems with $O3$ orientifold planes using the presence of $\frac{1}{2}$ D5-branes in neighbouring $\frac{1}{2}$ NS5-brane intervals. This rule is supported by various Hilbert series calculations matching moduli spaces across 3d mirror symmetry, which is realised as S-duality [20] in the brane systems under consideration.

Somewhat in parallel is the introduction of a set of identities between the Coulomb branches of a family of framed orthosymplectic gauge theories. Under certain conditions, these swap gauge nodes of B -type with those of type $O(2n)$ (along with a compensating change in flavour nodes). Using the aforementioned $O(2n)$ vs $SO(2n)$ rule, these identities are conjectured to have the interpretation of a Higgsing procedure that leaves the Coulomb branch invariant — in a brane system, this can be identified as a Kraft-Procesi transition on the $\frac{1}{2}$ D3-branes created when a D5-brane splits on an $\widetilde{O3^-}$ plane [23]. From the point of view of the Higgs branch Hasse diagram, this transition is conjectured to occur between two leaves that form part of the same special piece. ³

This note also conjectures an identity relating the Coulomb branches of the ‘ BC -’ and ‘ CB -chain’ quivers, defined in Section 5. Like the other conjectures in this note, this identity is supported via an explicit monopole formula calculation at the level of the unrefined Hilbert series. This Coulomb branch map can be performed in conjunction with those of Section 4.

Lastly, this note introduces a further conjecture regarding magnetic lattice gaugings and their emergence from brane systems. Using a conjecture regarding the behaviour of \mathbb{Z}_2 flavour symmetry gaugings in $\mathrm{Sp}(k)$ SQCD under 3d mirror symmetry, a rule is introduced for reading diagonal \mathbb{Z}_2 quotients on magnetic lattices from D3-/D5-/NS5-brane systems with $O3$ orientifold planes, which is checked explicitly.

²We thank Gwyn Bellamy and Travis Schedler for communicating their results.

³In fact, it implies a stronger statement. Namely, that the two leaves map to the same leaf under symplectic duality.

2 Brane and Quiver Conventions

The brane systems in this note consist of D3-branes suspended between D5- and NS5-branes in the presence of $O3$ orientifold planes. Their spacetime occupancy, given in Figure 1, leaves the threebranes free to extend through the x^6 dimension while the D5- and NS5-branes are infinite in the $x^{3,4,5}$ and $x^{7,8,9}$ directions respectively. In brane diagrams, the various $O3$ planes will be notated as in Table 1 —

	x^0	x^1	x^2	x^3	x^4	x^5	x^6	x^7	x^8	x^9
NS5	•	•	•	•	•	•				
D5	•	•	•					•	•	•
D3/ $O3$	•	•	•				•			

Figure 1: The Type IIB configurations in this note consist of D3-branes suspended between D5-branes and/or NS5-branes, together with orientifold planes at the origin.

$O3^\pm$ are exchanged across $\frac{1}{2}$ NS5-branes while $\frac{1}{2}$ D5-branes interchange tilded and untilded orientifolds. S -duality interchanges $O3^+$ and $\widetilde{O3^-}$, leaving $O3^-$ and $\widetilde{O3^+}$ untouched. Further information regarding the brane configurations used in this paper can be found in [4, 5, 23, 28].

Orientifold Plane	Brane Diagram	Electric Gauge Algebra	Magnetic Gauge Algebra
$O3^+$	-----	\mathfrak{c}	\mathfrak{b}
$\widetilde{O3^+}$	\mathfrak{c}	\mathfrak{c}
$\widetilde{O3^-}$	_____	\mathfrak{b}	\mathfrak{c}
$O3^-$		\mathfrak{d}	\mathfrak{d}

Table 1: The identification of gauge algebras from $O3$ -planes and brane diagram conventions. Switching from the electric to magnetic gauge algebra involves S-duality.

2.1 Quiver Derivation Rules

Given a D3-/D5-/NS5-brane system described in the previous section, the following rules identify the orthosymplectic quiver corresponding to the low energy worldvolume theory on the D3-branes. Table 1 is of course well-known and is included only for completeness. (Similarly, rules regarding flavours are widely used in [5, 23].)

- Given an interval between two $\frac{1}{2}$ NS5-branes containing both an $O3^+/\widetilde{O3^+}/\widetilde{O3^-}$ plane and a collection of D3-branes, the gauge algebra of the corresponding quiver gauge node is of the form given in Table 1.
- In general, $\frac{1}{2}$ D5-branes on the $O3$ orientifold planes contribute flavours in the corresponding quiver. The diagrams below give derivation rules for gauge nodes and flavours for D3-branes on various $O3$ orientifold planes. The dictionary given by (2.1), (2.2), (2.3) and (2.4) is well-known

from [5, 23].

(2.1)

(2.2)

(2.3)

(2.4)

- As has already been mentioned, the interpretation of D -type gauge nodes is more subtle than the $A - /B - /C -$ cases. Modulo O/SO ambiguities, $SO(2n)$ gauge groups are read from brane systems as shown in (2.5). Section 2.2 will consider this in further detail.

(2.5)

Semi-Infinite $\widetilde{O3}^-$ Planes A further condition exists for brane systems with semi-infinite $\widetilde{O3}^-$ planes of the sort seen in Figure 2. The naïve quiver derivation would result in a theory with a Witten anomaly [32] from the C -type gauge node seeing an odd number of half-hypers.

To amend this, it is useful to imagine the $\widetilde{O3}^-$ plane ending at infinity on a $\frac{1}{2}D5$ -brane. This can then be brought in and HW-transitioned as shown in Figure 2, removing the $\widetilde{O3}^-$ plane from the brane system and resulting in a non-anomalous quiver [23]. Note that this HW-transition is the only such allowed that neither creates nor annihilates $D3$ -branes — put simply, the trick given in Figure 2 would not work for semi-infinite $O3$ planes of any other type.

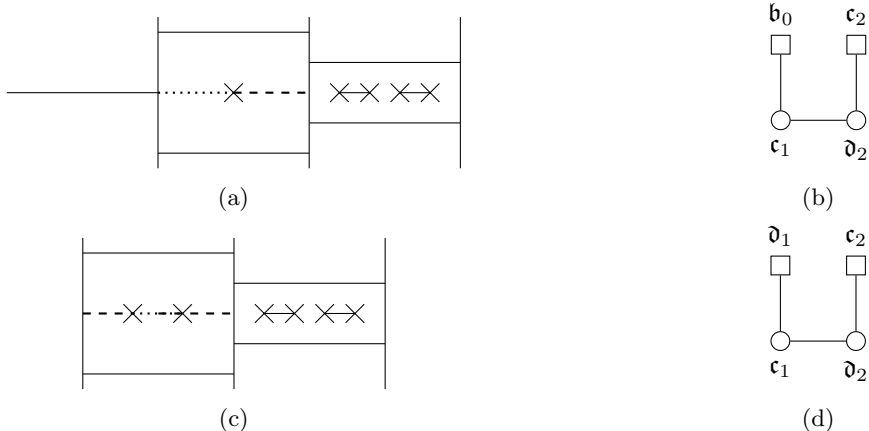


Figure 2: The brane system of Figure 2a does not give the anomalous theory in Figure 2b. After bringing in a $\frac{1}{2}$ D5-brane from infinity and performing an HW-transition, obtaining the brane system in Figure 2, the non-anomalous quiver Figure 2d is read.

2.2 $O(2n)$ versus $SO(2n)$

As mentioned in the previous section, reading the global form of the gauge group for gauge nodes with D -type algebras is unreliable. Appealing to past examples in [5], as well as a further simple example considered here, this section conjectures that the correct global form of a gauge node with D -type algebra is controlled by the presence of $\frac{1}{2}$ D5-branes on the $O3^+$ planes either side of the interval. The prescription is as follows.

- If there are zero D5-branes on either side of the interval, the gauge group $SO(2\ell)$ is read from ℓ D3-branes suspended between the two $\frac{1}{2}$ NS5-branes as in (2.5).
- If a single $\frac{1}{2}$ D5-brane is present on either side of the interval, the gauge group $O(2\ell)$ is read and the two C -type gauge nodes on either side pick up \mathfrak{b}_0 flavours as in (2.6). Multiple $\frac{1}{2}$ D5-branes on the $O3^+$ planes on either side of the $O3^-$ interval will also give rise to an $O(2\ell)$ gauge node, with flavours on the two C -type gauge nodes consistent with (2.2) and (2.3).

$$\begin{array}{c}
 n \quad \quad \quad \ell \quad \quad \quad m \\
 \cdot \times \text{---} \quad \quad \quad \text{---} \times \cdot \\
 \text{---} \quad \quad \quad \text{---} \quad \quad \quad \text{---}
 \end{array}
 \longleftrightarrow
 \begin{array}{c}
 \mathfrak{b}_0 \quad \quad \quad \mathfrak{b}_0 \\
 \square \quad \quad \quad \square \\
 | \quad \quad \quad | \\
 \cdots \text{---} \circ \text{---} \text{---} \text{---} \circ \text{---} \text{---} \text{---} \circ \text{---} \cdots \\
 \mathfrak{c}_n \quad \quad \quad O(2\ell) \quad \quad \quad \mathfrak{c}_m
 \end{array}
 \tag{2.6}$$

Example 1: Next-to-Minimal $SO(2n + 1)$ One of the most straightforward examples concerns the quiver (2.7), derived from the brane system in Figure 3, whose Coulomb branch is the closure of the next-to-minimal orbit of $SO(2k + 1)$, $\overline{O}_{(3,1^{2k-2})}^{B_k}$ [5].

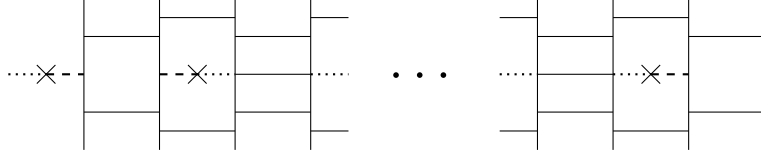
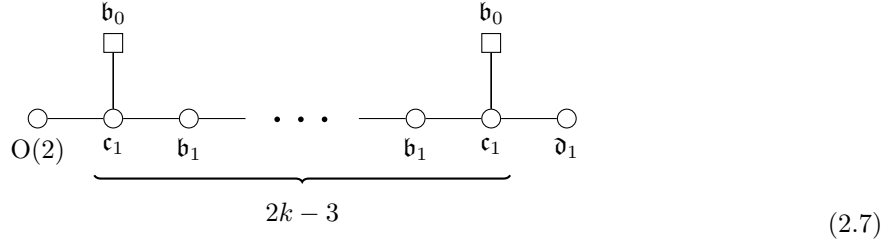


Figure 3: The brane system giving rise to the quiver (2.7), whose Coulomb branch is $\overline{\mathcal{O}}_{(3,1^{2k-2})}^{B_k}$ and whose Higgs branch is D_{k+1} [5]. The presence of the $\frac{1}{2}$ D5-brane on the far left is conjectured to gauge a \mathbb{Z}_2 resulting in the leftmost D -type gauge node of (2.7) becoming $O(2)$.



The Higgs and Coulomb branches of the corresponding 3d mirror, given in Figure 4b and derived

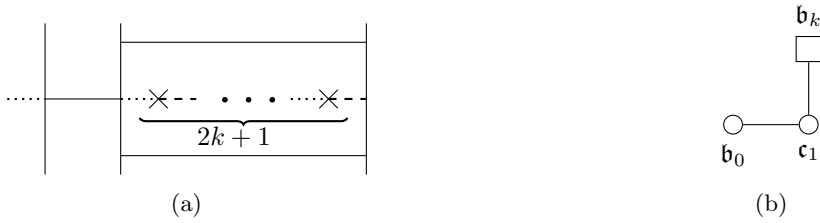


Figure 4: The brane system in Figure 4a, reached after performing S -duality on that given in Figure 3, gives rise to the quiver in Figure 4b.

from the brane system in Figure 4a, are $\overline{\mathcal{O}}_{(3,1^{2k-2})}^{B_k}$ and D_{k+1} (which is the top slice in the nilcone of \mathfrak{c}_k [17]) respectively. Without the \mathbb{Z}_2 gauging sending $SO(2)$ to $O(2)$ in (2.7), the moduli spaces of (2.7) would not match those of the dual (4b) derived from the brane system. This is one of the simplest cases wherein the \mathbb{Z}_2 quotient plays a crucial role in determining the resulting moduli spaces.

Example 2: Consider the brane system given in Figure 5a. Using the rule in (2.6), the gauge node with D -type gauge algebra should be read as $O(2)$ instead of $SO(2)$ – both possibilities are given in Figure 5b. Performing S -duality on the brane system to derive the 3d mirror theory results in the configuration given in Figure 5c, which unambiguously gives the corresponding quiver Figure 5d. The Coulomb branch of Figure 5d is insensitive to the \mathfrak{b}_0 gauging and in Figure 5a both $G = SO(2)$ and $G = O(2)$ give the same Higgs branch [31]. Hence it is the Coulomb branch of Figure 5b and the Higgs branch of Figure 5d which provide the nontrivial check. The Hilbert series for the Higgs branch of Figure 5d is given in (2.8). Upon computing the Coulomb branches of the two candidate quivers in Figure 5b, only the quiver with the $O(2)$ gauge node gives the same (unrefined) Hilbert series as (2.8), shown in (2.9). In the brane system Figure 5a, this agrees with the presence of $\frac{1}{2}$ D5-branes either side

of the leftmost $\frac{1}{2}$ NS5-brane interval.

$$\text{HS}_{\mathcal{H}}(\mathcal{Q}_{5d}) = \frac{\text{PE} [([4] - [2]) t^4]}{\times (1 + [2] t^2 + (2[2] + [1]) t^4 + ([4] + [2] + 2[1]) t^6 + \dots + t^{12})} \quad (2.8)$$

$$\text{HS}_{\mathcal{H}}(\mathcal{Q}_{5d})|_{a,b \rightarrow 1} = \frac{1 + t^2 + 4t^4 + t^6 + t^8}{(1 - t^2)^2 (1 - t^4)^2} = \text{HS}_{\mathcal{C}}(\mathcal{Q}_{5a}|_{G=O(2)}) \quad (2.9)$$

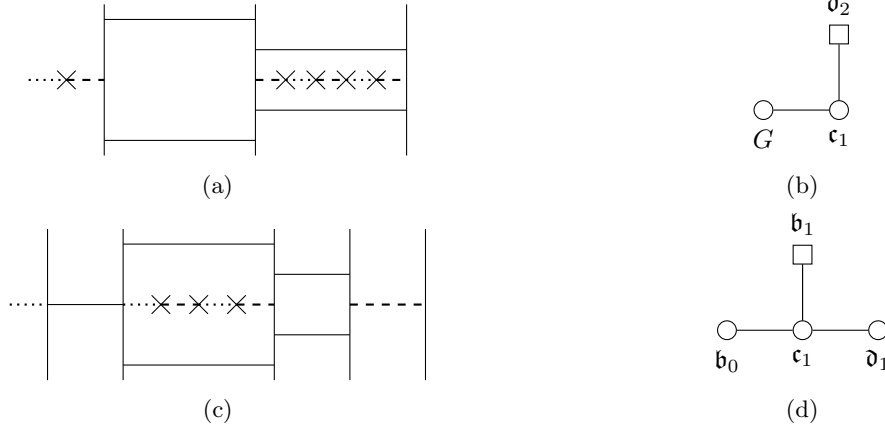


Figure 5: The leftmost $\frac{1}{2}$ NS5-brane interval in the brane system in Figure 5a can be argued to give rise to either a $G = \text{SO}(2)$ or a $G = \text{O}(2)$ gauge node. It turns out that only $G = \text{O}(2)$ is the consistent choice. Figure 5c gives the brane system obtained from Figure 5a after S-duality, the resulting theory is given in Figure 5d.

Lusztig’s Canonical Quotient Many examples of the phenomenon considered in (2.6) can be found in [28]. In these cases, the presence of a \mathbb{Z}_2 gauging implied the existence of an $\bar{A}(\mathcal{O}) = \mathbb{Z}_2$ canonical quotient [25, 26, 33] on the Coulomb branch. Of course, given that (2.6) ascribes a \mathbb{Z}_2 quotient to a relatively arbitrary brane system – crucially, one whose associated Coulomb branch is not necessarily a nilpotent orbit closure – the question arises as to the interpretation of this finite group data *outside* the nilcone.

$$\begin{array}{cccccccccccc} \circ & \circ & \circ & \circ & \circ & \circ & \circ & \circ & \square & \circ & \circ & \circ & \circ \\ \partial_1 & c_1 & \partial_2 & c_2 & \partial_3 & c_3 & \partial_4 & c_4 & \partial_1 & \text{O}(8) & c_3 & \text{O}(4) & \\ \end{array} \quad (2.10)$$

Following [28], the canonical quotient of Lusztig (LCQ) associated to a nilpotent orbit closure is read from a framed orthosymplectic quiver by considering the number of \mathbb{Z}_2 gaugings applied to nodes with D -type algebras. For instance, the $T_{[4^2, 2^2]}(\text{Sp}(6))$ theory in (2.10), whose Coulomb branch is $\bar{\mathcal{O}}^{[5, 3^2, 1^2]}$ in the nilpotent cone of \mathfrak{so}_{13} [28] has $\bar{A}(\mathcal{O}) = (\mathbb{Z}_2)^2$ – one \mathbb{Z}_2 from each gauge node of the form $\text{O}(2\ell)$. Diagonally-gauged SO-nodes – to be considered further in Section 6 – similarly contribute a single

\mathbb{Z}_2 . In the language of [28], the LCQ of a quiver whose Coulomb branch is a nilpotent orbit closure is $(\mathbb{Z}_2)^m$, where m is the number of ‘chains’ in the quiver.

Although the LCQ is read differently in the case of unitary quivers to the rule given here, the generality of these quiver constructions leads to the question of extending the definition of the LCQ outside nilpotent cones. It is tempting to conjecture that the Coulomb branch of any framed orthosymplectic quiver with gauged \mathbb{Z}_2 factors induced by chains has some analogue of an LCQ given as $(\mathbb{Z}_2)^k$, where k is the number of chains.⁴ Moreover, it would be interesting to consider if such an argument could be extended to decorations of arbitrary sub-quivers giving isolated singularities, making the connection with gauging finite symmetries clearer.

3 A Motivating Example: $O(3)$ with N_f Flavours

One of the simplest examples of the manipulations studied in this work concerns $O(3)$ gauge theory with N_f flavours rotated under $\text{Sp}(N_f)$. The Higgs branch is well known to be the closure of the nilpotent orbit $[2^3, 1^{2n-6}]$, with Hasse diagram as given in Figure 6. In a brane system, the $O(3)$ gauge theory can be realised as in Figure 7a, where the $\frac{1}{2}\text{D5}$ -branes are split along the $O3$ orientifolds. Higgsing the theory corresponds to performing a Kraft-Procesi transition on the $\frac{1}{2}\text{D3}$ -branes created between $\frac{1}{2}\text{D5}$ -branes on $\widetilde{O3^-}$ planes, highlighted in red in Figure 7b; after X-collapse, the brane system is as shown in Figure 7c – naively, this would be interpreted as an $\text{SO}(2)$ gauge theory with $N_f - 1$ flavours. However, in accordance with the rule given in Section (2.6), the gauge group is instead read as $O(2)$. This agrees with the field theory, which stipulates that the Higgsing returns an $O(2)$ gauge theory.

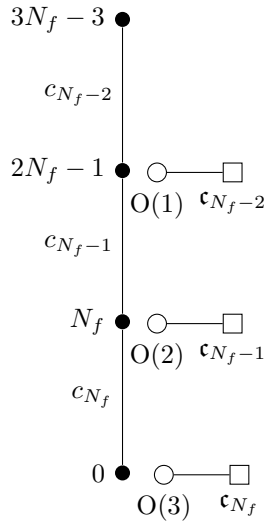


Figure 6: The Hasse diagram for the Higgs branch of $O(3)$ gauge theory with N_f flavours, with leaves labelled by their dimension alongside the Higgsing pattern down to $O(1)$ gauge theory with $N_f - 2$ flavours.

⁴Similarly, it can be conjectured that the Coulomb branch of any decorated unframed quiver (unitary or orthosymplectic) has an associated S_n ‘Lusztig canonical quotient’ corresponding to the number of decorated gauge nodes of rank 1 [15, 34, 35].

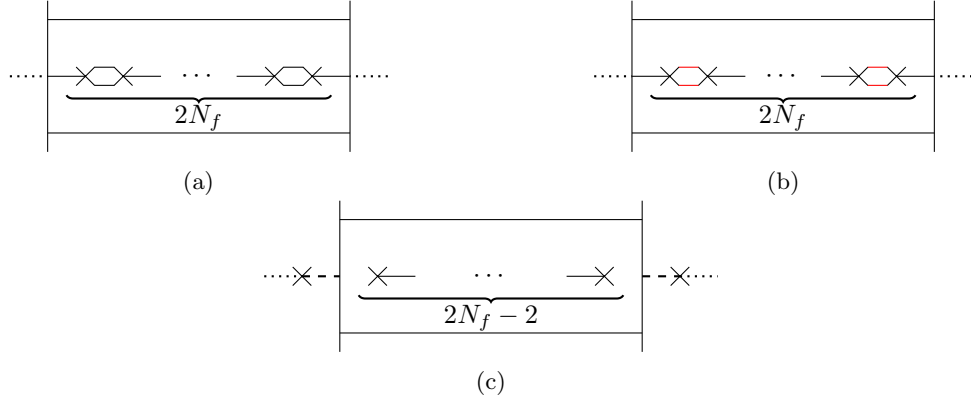


Figure 7: The Higgsing process taking the $O(3)$ gauge theory with N_f flavours, read from the brane system in Figure 7a, to the $O(2)$ gauge theory with $N_f - 1$ flavours. The $\frac{1}{2}$ D3-branes created under the splitting of a D5-brane on an $\widehat{O3}^-$ plane, represented in red in Figure 7b, undergo a Kraft-Procesi transition resulting in the brane system in Figure 7c, from which the $O(2)$ gauge theory is read. Note that this is $O(2)$ instead of $SO(2)$, as given in the rule in (2.6).

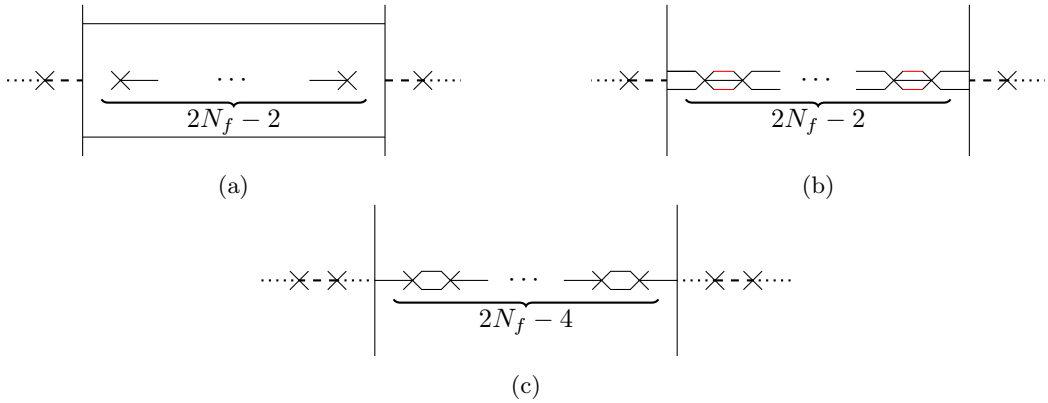


Figure 8: The Higgsing process taking the $O(2)$ gauge theory with $N_f - 1$ flavours, read from the brane system in Figure 8a, to the $O(1)$ gauge theory with $N_f - 2$ flavours in Figure 8c. Splitting the $\frac{1}{2}$ D3-brane along the fivebranes, shown in Figure 8b, allows for the segments coloured red to be ‘removed’ under the Kraft-Procesi transition, which gives a brane interpretation of the lost $N_f - 1$ moduli. The remaining segments either play the role of moduli or, in the case of the $\frac{1}{2}$ D3-branes suspended between the $\frac{1}{2}$ NS5-branes and $\frac{1}{2}$ D5-branes, can be annihilated under a Hanany-Witten transition.

Importantly, the branes involved in the Kraft-Procesi transition, shown in Figure 7b, locally support an $O(1)$ gauge theory with N_f flavours, whose Higgs branch is the closure of the minimal nilpotent orbit of $Sp(N_f)$. Further Higgsing of the theory can be realised in the brane system via the Kraft-Procesi transition shown in Figure 8; splitting the $\frac{1}{2}$ D5-branes and performing a Hanany-Witten transition results in the brane system in Figure 8c, which supports an $O(1)$ gauge theory with $N_f - 2$ flavours. Clearly, this agrees with the field theory Hasse diagram given in Figure 6.

Now consider the Coulomb branches of the $O(3)$ and $O(2)$ gauge theories given here. It is straight-

forward to show using the monopole formula [36, 37],

$$\text{HS}(t) = \sum_{m \in \Gamma_{\mathcal{W}}^{\mathcal{G}_V}} P_G(t; m) t^{2\Delta(t; m)}, \quad (3.1)$$

that both spaces have identical unrefined Hilbert series. Since the magnetic charges associated to $O(2k)$ and $SO(2k + 1)$ take values on the same lattice (and the two groups have the same dressing factor P_G) it is sufficient to check that the conformal dimensions of the two quivers are the same. A simple calculation shows that in both cases $\Delta = (n - 2) |m|$ where m is the magnetic charge associated to (each) gauge group. As such, the unrefined Hilbert series of the Coulomb branches of the $O(3)$ and $O(2)$ gauge theories in Figure 6 coincide. Although this is not conclusive evidence that the two moduli spaces are in fact identical, it is significant evidence towards this conclusion. For this reason, results of this kind are used throughout this paper to motivate conjectures of Coulomb branch equivalence.

This example is included to provide a context for the manipulations performed in the rest of this paper. Using Kraft-Procesi transitions of the kind evidenced here between the $O(3)$ and $O(2)$ gauge theories, a set of identities on the Coulomb branches of various quivers can be found that, under certain conditions, swap $SO(2k + 1)$ and $O(2k)$ gauge groups along with a compensating change to flavours. These transformations have the interpretation of a Higgsing that keeps the Coulomb branch invariant which, from the perspective of the Hasse diagram, motivates the conjecture that the theories related by the Higgsing form part of the same special piece [25, 26, 33, 38, 39].

4 The $B_n \leftrightarrow O(2n)$ Identity

The observation in Section 3 that the $O(3)$ and $O(2)$ gauge theories have the same Coulomb branch can be understood in terms of a broader set of Coulomb branch identities. These concern linear orthosymplectic quivers with a framed B -type node between two framed nodes of C -type. A similar argument to that given in Section 3 shows the unrefined Hilbert series of the quivers' Coulomb branches to be identical, motivating the conjecture that the moduli spaces themselves are the same. As in Section 3, the Coulomb branch identities introduced in this section are conjectured to admit a brane interpretation as a Higgsing inside a special piece. Performing a Kraft-Procesi transition on the D3-branes created when a D5-brane splits along an $\widetilde{O3}^-$ plane makes the link between the two theories manifest, and provides further justification for the rule given in Section 2.2.

Consider the theory given on the left in (4.1). The general type of manipulation considered in this section consists in changing the \mathfrak{b}_k gauge node into the $O(2k)$ node shown on the right-hand side. Alongside a compensating change to the flavour groups F_1 and F_2 , this action is conjectured to leave the Coulomb branch invariant. Current methods limit confidence in this conjecture to the unrefined Hilbert series, which is shown explicitly in Appendix A to remain invariant. Although the intuition behind (4.1) is made clearest using the brane interpretation given in Section 4.1, the following considers a few generic examples.

In the examples below, the

$$\begin{array}{ccc}
 \begin{array}{c} O(r_1) \\ \square \\ | \\ \circ \\ \mathfrak{c}_{k_1} \end{array} & \begin{array}{c} \mathfrak{c}_{k_2} \\ \square \\ | \\ \circ \\ \mathfrak{b}_k \end{array} & \begin{array}{c} O(r_2) \\ \square \\ | \\ \circ \\ \mathfrak{c}_{k_3} \end{array} \\
 \dots & \text{---} & \dots
 \end{array}
 \quad \stackrel{\mathcal{C}}{=} \quad
 \begin{array}{ccc}
 \begin{array}{c} O(r_1 + 1) \\ \square \\ | \\ \circ \\ \mathfrak{c}_{k_1} \end{array} & \begin{array}{c} \mathfrak{c}_{k_2 - 1} \\ \square \\ | \\ \circ \\ O(2k) \end{array} & \begin{array}{c} \square \\ | \\ \circ \\ \mathfrak{c}_{k_3} \end{array} \\
 \dots & \text{---} & \dots
 \end{array}
 \quad (4.1)$$

Examples

- $r_1 = 2m, r_2 = 2n + 1$: One such example involves the two quivers in (4.2). Replacing the central \mathfrak{b}_k gauge node with $O(2k)$ maintains the Coulomb branch as long as the flavours of the three gauge nodes are amended as shown. In the example in (4.2), the two C -type gauge nodes on either side see different flavour groups — the identity remains valid if the two flavour groups are of the same type (in other words, the flavour groups of the two C -type gauge nodes could both be of type D or type B - the example in (4.2) is included to illustrate how each of the D - and B -type flavours change).

$$\begin{array}{ccc}
 \begin{array}{c} \mathfrak{d}_m \\ \square \\ | \\ \circ \\ \mathfrak{c}_{k_1} \end{array} & \begin{array}{c} \mathfrak{c}_{k_2} \\ \square \\ | \\ \circ \\ \mathfrak{b}_k \end{array} & \begin{array}{c} \mathfrak{b}_n \\ \square \\ | \\ \circ \\ \mathfrak{c}_{k_3} \end{array} \\
 \dots & \text{---} & \dots
 \end{array} \quad \stackrel{\mathcal{C}}{=} \quad \begin{array}{ccc}
 \begin{array}{c} \mathfrak{b}_m \\ \square \\ | \\ \circ \\ \mathfrak{c}_{k_1} \end{array} & \begin{array}{c} \mathfrak{c}_{k_2-1} \\ \square \\ | \\ \circ \\ O(2k) \end{array} & \begin{array}{c} \mathfrak{d}_{n+1} \\ \square \\ | \\ \circ \\ \mathfrak{c}_{k_3} \end{array} \\
 \dots & \text{---} & \dots
 \end{array} \quad (4.2)$$

- $r_1 = r_2 = 1$: The $m = n = 0$ case is an illustrative example in which the \mathfrak{b}_0 nodes on either side of the central $SO(2k + 1)$ gauge node are promoted to \mathfrak{d}_1 .

$$\begin{array}{ccc}
 \begin{array}{c} \mathfrak{b}_0 \\ \square \\ | \\ \circ \\ \mathfrak{c}_{k_1} \end{array} & \begin{array}{c} \mathfrak{c}_{k_2} \\ \square \\ | \\ \circ \\ \mathfrak{b}_k \end{array} & \begin{array}{c} \mathfrak{b}_0 \\ \square \\ | \\ \circ \\ \mathfrak{c}_{k_3} \end{array} \\
 \dots & \text{---} & \dots
 \end{array} \quad \stackrel{\mathcal{C}}{=} \quad \begin{array}{ccc}
 \begin{array}{c} \mathfrak{d}_1 \\ \square \\ | \\ \circ \\ \mathfrak{c}_{k_1} \end{array} & \begin{array}{c} \mathfrak{c}_{k_2-1} \\ \square \\ | \\ \circ \\ O(2k) \end{array} & \begin{array}{c} \mathfrak{d}_1 \\ \square \\ | \\ \circ \\ \mathfrak{c}_{k_3} \end{array} \\
 \dots & \text{---} & \dots
 \end{array} \quad (4.3)$$

- $r_1 = r_2 = 0$: This example illustrates the case in which both C -type nodes beside the central B -type node are initially unframed. Performing the transition causes them to pick up a \mathfrak{b}_0 framing — the rank of the flavour group associated to the central B -type gauge node decreases by one.

$$\begin{array}{ccc}
 & \begin{array}{c} \mathfrak{c}_{k_2} \\ \square \\ | \\ \circ \\ \mathfrak{b}_k \end{array} & \\
 \dots & \text{---} & \dots
 \end{array} \quad \stackrel{\mathcal{C}}{=} \quad \begin{array}{ccc}
 \begin{array}{c} \mathfrak{b}_0 \\ \square \\ | \\ \circ \\ \mathfrak{c}_{k_1} \end{array} & \begin{array}{c} \mathfrak{c}_{k_2-1} \\ \square \\ | \\ \circ \\ O(2k) \end{array} & \begin{array}{c} \mathfrak{b}_0 \\ \square \\ | \\ \circ \\ \mathfrak{c}_{k_3} \end{array} \\
 \dots & \text{---} & \dots
 \end{array} \quad (4.4)$$

As the above examples show, the general pattern for the flavours F_1 and F_2 in (4.1) is $SO(r) \rightarrow SO(r + 1)$. Alongside the diminution in rank of the \mathfrak{c}_{k_2} flavour node, this hints at the possibility of interpreting the identity (4.1) in terms of a process in a brane system, explored further in the next section.

4.1 As a Higgsing

Interpreting the conjectures of the previous section in terms of branes follows broadly the same logic as in Section 3. Like before, the two quivers' equivalent Coulomb branches are taken in the brane

system to point towards a Higgsing between them that remains inside the same special piece in their Coulomb branch Hasse diagram. Consider for example the brane system given in Figure 9a, from which the quiver on the left in (4.2) can be read. Removing the $\frac{1}{2}$ -branes in red in Figure 9a under a Kraft-Procesi transition and performing an HW-transition on the left- and right-most $\frac{1}{2}$ D5-branes results in the brane configuration in Figure 9b. Using the derivation rule of Section 2.1, the central $\frac{1}{2}$ NS5-brane interval in Figure 9b appears to support an $O(2k)$ gauge theory, as on the right-hand side of (4.2). That the Higgsing in Figure 9 preserves the Coulomb branch can be argued from the fact

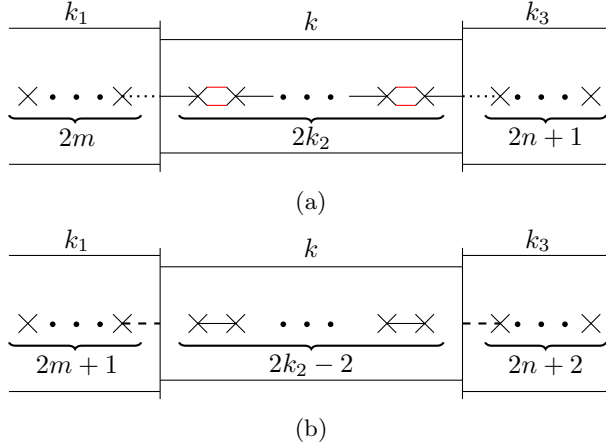


Figure 9: The Higgsing of the theory of (4.2) to that on the right. The red branes in Figure 9a are removed via the Kraft-Procesi transition and the two D5-branes closest to the NS5-branes are HW-transitioned into the neighbouring interval to recover the configuration in Figure 9b. The transition is c_{k_2} and is conjectured to be a ‘special Higgsing’ (note that this terminology is not standard and is not desired for wider use) that remains in the same special piece in the Higgs branch Hasse diagram.

that no Coulomb branch moduli appear to be lost in the brane system. Note that this is only the case if the gauge node with D -type algebra is interpreted as $O(2k)$ instead of $SO(2k)$, in line with the proposal of Section 2.2.

The phenomenon is essentially the same in the case of (4.3) and (4.4). For (4.4), the brane realisation is given in Figure 10. The Kraft-Procesi transition deposits a single $\frac{1}{2}$ D5-brane into each of the left- and right-hand side $\frac{1}{2}$ NS5-brane intervals, as reflected in the \mathfrak{b}_0 flavours.

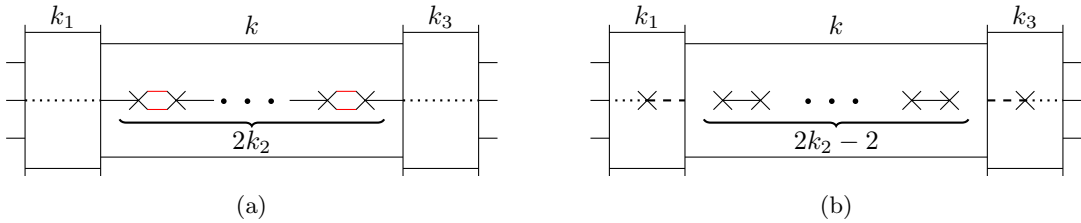


Figure 10: The brane interpretation of the identity in (4.4). In Figure 10a, which corresponds to the theory on the left of (4.4), the red branes are removed under a Kraft-Procesi transition. Rearranging the brane system using an HW-transition results in that given in Figure 10b. Using the rule in Section 2.2, the central NS5-brane interval is interpreted as supporting an $O(2k)$ gauge theory. The placements of the $\frac{1}{2}$ D5-branes exactly correspond to the flavours on the right hand side of (4.4).

4.2 Special Piece Generalisation

As remarked in Section 2.2 and [28], in quivers whose Coulomb branch corresponds to a nilpotent orbit closure in the nilcone of a $B/C/D$ -type algebra, the appearance of $O(2n)$ instead of $SO(2n)$ in gauge nodes can be identified with factors of \mathbb{Z}_2 in the Lusztig canonical quotient associated to the leaf.

5 The BC - and CB -Chains

$$(5.1)$$

Another identity introduced in this note concerns the BC - and CB -chain quivers in (5.1). The Coulomb branch, which is shared by both quivers, is of dimension $k(2N + 1)$ and has global symmetry $SO(2N + 2)$ – Coulomb branch Hilbert series for various examples are given in Appendix B.

Like the identities proposed in Section 4, the equivalence of the two Coulomb branches in (5.1) can be demonstrated at the level of unrefined Hilbert series using the monopole formula [36], which calculates the Hilbert series for a moduli space of dressed monopole operators using a quiver’s conformal dimension $\Delta(t; m)$, gauge group-dependent dressing factors $P_G(t; m)$ and magnetic lattice Weyl orbits $\Gamma_{\mathcal{W}}^{G_V}$. Since magnetic lattices and dressing factors are identical for both B - and C -type groups, to check the conjecture (5.1) at the level of unrefined Hilbert series it suffices to match the two conformal dimensions. In Figure 11, (5.1) is rewritten alongside the magnetic charges associated to each gauge group. First consider the CB -chain in Figure 11a with conformal dimension Δ_L given in (5.6).

(a) (b)

Figure 11: Figure 11a gives the CB -quiver with $N + 1$ gauge nodes of C -type and N gauge nodes of B -type and Figure 11b gives the BC -quiver with $N + 1$ gauge nodes of B -type and N gauge nodes of C -type. The tuple of magnetic charges associated to each gauge node is given below the algebra label — in Figure 11a C - and B -type nodes have charges of the form m_i^α and n_i^α respectively while in Figure 11b they are labelled by h_i^α and g_i^α .

$$\Delta_L^{\text{Hyp}} = k \sum_{i=1}^k |m_i^1| + k \sum_{i=1}^k |m_i^{N+1}| + \frac{1}{2} \sum_{\alpha=1}^N \sum_{i,j=1}^k (|m_i^\alpha + n_j^\alpha| + |m_i^\alpha - n_j^\alpha|) + \sum_{\alpha=1}^{N+1} \sum_{i=1}^k |m_i^\alpha| \quad (5.2)$$

$$+ \frac{1}{2} \sum_{\alpha=1}^N \sum_{i,j=1}^k (|n_i^\alpha + m_j^{\alpha+1}| + |n_i^\alpha - m_j^{\alpha+1}|) \quad (5.3)$$

$$\Delta_L^{\text{Vec}} = - \sum_{\alpha=1}^{N+1} \sum_{i<j}^k (|m_i^\alpha + m_j^\alpha| + |m_i^\alpha - m_j^\alpha|) - \sum_{\alpha=1}^N \sum_{i<j}^k (|n_i^\alpha + n_j^\alpha| + |n_i^\alpha - n_j^\alpha|) \quad (5.4)$$

$$- 2 \sum_{\alpha=1}^{N+1} \sum_{i=1}^k |m_i^\alpha| - \sum_{\alpha=1}^N \sum_{i=1}^k |n_i^\alpha| \quad (5.5)$$

$$\Delta_L = \Delta_L^{\text{Hyp}} + \Delta_L^{\text{Vec}} = \Sigma_{m,n} - \sum_{\alpha=2}^N \sum_{i=1}^k |m_i^\alpha| - \sum_{\alpha=1}^N \sum_{i=1}^k |n_i^\alpha| + (k-1) \sum_{i=1}^k (|m_i^1| + |m_i^{N+1}|) \quad (5.6)$$

Note that $\Sigma_{m,n}$ is a repackaging of terms of the form $|m \pm n|$, $|m_i \pm m_j|$ and $|n_i \pm n_j|$. The BC -chain in Figure 11b with conformal dimension Δ_R proceeds analogously (5.11).

$$\Delta_R^{\text{Hyp}} = k \sum_{i=1}^k |g_i^1| + k \sum_{i=1}^k |g_i^{N+1}| + \sum_{\alpha=1}^N \sum_{i=1}^k |h_i^\alpha| + \frac{1}{2} \sum_{\alpha=1}^N \sum_{i,j=1}^k (|g_i^\alpha + h_j^\alpha| + |g_i^\alpha - h_j^\alpha|) \quad (5.7)$$

$$\frac{1}{2} \sum_{\alpha=1}^N \sum_{i,j=1}^k (|h_i^\alpha + g_j^{\alpha+1}| + |h_i^\alpha - g_j^{\alpha+1}|) \quad (5.8)$$

$$\Delta_R^{\text{Vec}} = - \sum_{\alpha=1}^{N+1} \sum_{i<j}^k (|g_i^\alpha + g_j^\alpha| + |g_i^\alpha - g_j^\alpha|) - \sum_{\alpha=1}^N \sum_{i<j}^k (|h_i^\alpha + h_j^\alpha| + |h_i^\alpha - h_j^\alpha|) \quad (5.9)$$

$$- 2 \sum_{\alpha=1}^N \sum_{i=1}^k |h_i^\alpha| - \sum_{\alpha=1}^{N+1} \sum_{i=1}^k |g_i^\alpha| \quad (5.10)$$

$$\Delta_R = \Delta_R^{\text{Hyp}} + \Delta_R^{\text{Vec}} = \Sigma_{g,h} - \sum_{\alpha=2}^N \sum_{i=1}^k |g_i^\alpha| - \sum_{\alpha=1}^N \sum_{i=1}^k |h_i^\alpha| + (k-1) \sum_{i=1}^k (|g_i^1| + |g_i^{N+1}|) \quad (5.11)$$

Where again $\Sigma_{g,h}$ packages terms of the form $|g \pm h|$, $|g_i \pm g_j|$ and $|h_i \pm h_j|$. Since (m^α, n^β) and (g^α, h^β) , for $\alpha = 1, \dots, N+1$, $\beta = 1, \dots, N$, are summed over the same lattice, the conformal dimension contributions of the two quivers in Figure 11a and Figure 11b are identical.

Note that the identities in Section 4 are also applicable to the BC -quiver given in (5.1). One such example is given in (5.12).

$$(5.12)$$

6 Gauging \mathbb{Z}_2 Flavour Subgroups of $\text{Sp}(k)$ SQCD

In three dimensions, the Higgs branch of SQCD with gauge group $\text{Sp}(k)$ exhibits a range of different structures as N_f , the number of flavours, is varied. For instance, $N_f = 2k$ cleaves the Higgs branch into a union of two cones [40, 41] with global symmetry $\text{SO}(4k)$, while the Higgsing pattern for $N_f = 2k+1$

is a series of d_{2n+1} transitions. In this section, a set of Higgs and Coulomb branch relations will be presented for theories under the gauging of \mathbb{Z}_2 subgroups of their flavour symmetries.

$$\begin{array}{c}
 \mathfrak{d}_{N_f} \\
 \square \\
 | \\
 \circ \\
 \mathfrak{c}_k
 \end{array}
 \tag{6.1}$$

Consider the $\text{Sp}(k)$ SQCD with $N_f = 2k + 1$ in (6.1). Gauging successive \mathbb{Z}_2 subgroups (denoted \mathfrak{b}_0) of the flavour symmetry that act trivially on monopole operators leaves the Coulomb branch unchanged, as shown in (6.3).⁵ The embedding is specified as,

$$[1, 0, \dots, 0]_D \mapsto [1, 0, \dots, 0]_B + [0]_B,
 \tag{6.2}$$

where the first term on the right-hand side transforms trivially under \mathbb{Z}_2 and the second non-trivially. Such gaugings will generically change the Higgs branch. Using S-duality in a Type IIB brane system, this \mathbb{Z}_2 gauging is conjectured to be related under 3d mirror symmetry⁶ to gauging the diagonal \mathbb{Z}_2 lattice symmetry on a maximal DC -chain, as shown in Table 2. This conjecture is supported by matching Coulomb branch Hilbert series of the magnetic theories of Table 2 with those of the Higgs branches of the electric theories. The map between \mathbb{Z}_2 flavour gauging on the left-hand column and the diagonal \mathbb{Z}_2 on the right-hand column of Table 2 is in some sense reminiscent of [42]. Note that information on this sort of diagonal gauging can be found in [28].

$$\begin{array}{c}
 \mathfrak{d}_{2k+1} \\
 \square \\
 | \\
 \circ \\
 \mathfrak{c}_k
 \end{array}
 \stackrel{\mathcal{C}}{=}
 \left.
 \begin{array}{c}
 \mathfrak{d}_{2k+1-m} \\
 \square \\
 | \\
 \circ \\
 | \\
 \circ \\
 \vdots \\
 \circ \\
 | \\
 \circ \\
 \mathfrak{c}_k
 \end{array}
 \right\} 2m
 \stackrel{\mathcal{C}}{=}
 \left.
 \begin{array}{c}
 \mathfrak{b}_{2k-m} \\
 \square \\
 | \\
 \circ \\
 | \\
 \circ \\
 \vdots \\
 \circ \\
 | \\
 \circ \\
 \mathfrak{c}_k
 \end{array}
 \right\} 2m + 1
 \tag{6.3}$$

Like in Section 4.1, it is instructive to consider a brane interpretation of the diagonal gauging shown in Table 2. Take the initial brane configuration in Figure 12a corresponding to the electric theory in Figure 12b. Using a Type IIB brane system, the brane configuration can be related to the magnetic theory given in Figure 13, where now the $\frac{1}{2}$ NS5-brane on the left-hand side of Figure 12a has become a $\frac{1}{2}$ D5-brane. Using an analogue of the conjecture in Section 2.2, it appears that $\frac{1}{2}$ D5-branes book-ending a maximal DC -chain have the effect of diagonally gauging a \mathbb{Z}_2 lattice subgroup in the D3-brane

⁵It is possible to stipulate that monopole operators are charged under this \mathbb{Z}_2 , considered in [10]. In this case the Coulomb branch will generically change as new gauge-invariant combinations of monopole operators emerge. The authors thank Noppadol Mekareeya and William Harding for discussion on this point.

⁶Although Hilbert series checks suggest that the moduli spaces of the electric and magnetic theories in Table 2 obey a 3d mirror symmetry relationship, this alone is insufficient to conclude that the theories are strictly dual.

worldvolume theory, as shown in (6.4).

(6.4)

Gauging another \mathbb{Z}_2 flavour subgroup gives rise to a further $\frac{1}{2}$ D5-brane at the *other* end of the brane system in Figure 13. Using the rule of (6.4), this corresponds to gauging the diagonal \mathbb{Z}_2 in the other long *DC*-chain of the magnetic theory, which is supported in the field theory by calculating (unrefined) moduli space Hilbert series. The conjecture in (6.4) has several simple examples. For $k = 1$ and one

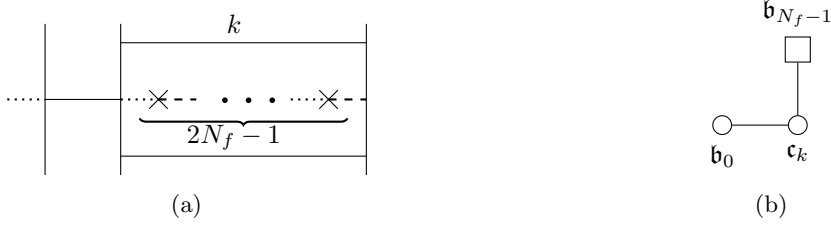


Figure 12: The brane system in Figure 12a gives rise to the quiver on the right in Figure 12b. The leftmost $\frac{1}{2}$ NS5-brane interval gives rise to the \mathbb{Z}_2 gauge node.

\mathbb{Z}_2 gauging the conjecture reduces to the next-to-minimal $\text{SO}(2\ell + 1)$ nilpotent orbit closure quivers given in [5]. For $k = 1$ with two \mathbb{Z}_2 gaugings the conjecture can be tested explicitly using unrefined Hilbert series. For $k = 2$ and one \mathbb{Z}_2 gauging the conjecture precisely replicates the results found in [28] for the closure of the $[3, 2^2, 1]$ orbit of \mathfrak{so}_9 .

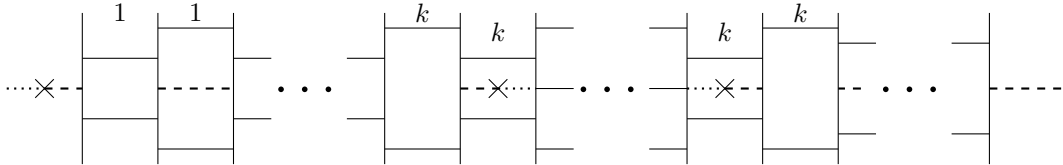


Figure 13: The brane system in Figure 13 is that of Figure 12a under rotation and S-duality. The leftmost NS5-brane in Figure 12a, which gives rise to the \mathbb{Z}_2 gauge symmetry, becomes the leftmost $\frac{1}{2}$ D5-brane in Figure 13. The corresponding quiver is conjectured to be the magnetic theory in the middle row of Table 2, where the presence of the extra $\frac{1}{2}$ D5-brane gives rise to the diagonal \mathbb{Z}_2 quotient.

6.1 Example

The rule given in (6.4) can be checked explicitly using the example in Figure 14. Under (6.4), the brane system in Figure 14a appears to yield the quiver with the diagonal \mathbb{Z}_2 gauging given in Figure 14b.⁷ By moving to the magnetic phase of the brane system, given in Figure 14c, the corresponding magnetic theory is unambiguously read as Figure 14d. Computing the (refined) Higgs branch Hilbert series of Figure 14c and the (unrefined) Coulomb branch Hilbert series of Figure 14b shows agreement, as seen in (6.6) and (6.5). As the diagonal gauging in Figure 14b does not affect the Higgs branch, so does the \mathbb{Z}_2 flavour subgroup gauging in Figure 14d leave the Coulomb branch invariant. As such, $\mathcal{H}(\mathcal{Q}_{14b}) = \mathcal{C}(\mathcal{Q}_{14d})$.

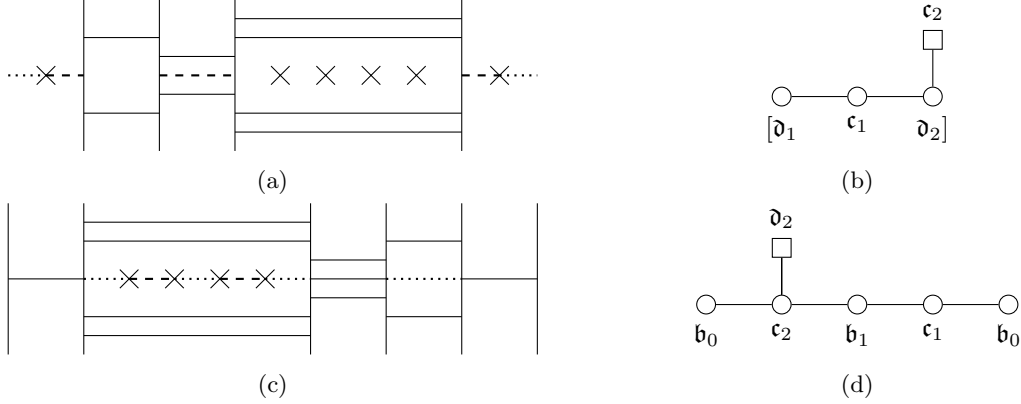


Figure 14: The brane system in Figure 14a yields the quiver Figure 14b under the application of the rule given in (6.4). The $\frac{1}{2}$ D5-branes at each end of the maximal chain gauge the diagonal \mathbb{Z}_2 symmetry on the magnetic lattice. The brane system in Figure 14c results from performing an S-duality transformation on that of Figure 14a. The associated theory, given in Figure 14b, is read unambiguously.

$$\text{HS}_{\mathcal{H}}(\mathcal{Q}_{14d}) = \text{PE} \left[([2; 0] + [0; 2])t^2 + ([2; 2] - [2; 0] - [2; 0] - 1)t^4 \right] \times (1 + t^4)(1 + ([2; 0] + [0; 2])t^4 + t^8) \quad (6.5)$$

$$\text{HS}_{\mathcal{H}}(\mathcal{Q}_{14d})|_{a,b \rightarrow 1} = \frac{(1 + t^4)(1 + 6t^4 + t^8)}{(1 - t^2)^6(1 - t^4)^2} = \text{HS}_{\mathcal{C}}(\mathcal{Q}_{14b}) \quad (6.6)$$

Hence, the moduli space calculations support the interpretation of Figure 7 and Figure 7 as a 3d mirror pair – note that without the diagonal \mathbb{Z}_2 gauging the Coulomb branch of Figure 7 would not match the Higgs branch of Figure 7. The interplay between diagonal \mathbb{Z}_2 quotients on magnetic lattices and \mathbb{Z}_2 flavour gaugings appears to be generic for this class of framed orthosymplectic theories.

⁷Note that the monopole formula for Figure 7 deviates from the un-gauged case solely in the dressing factor, following (6.15) in [28].

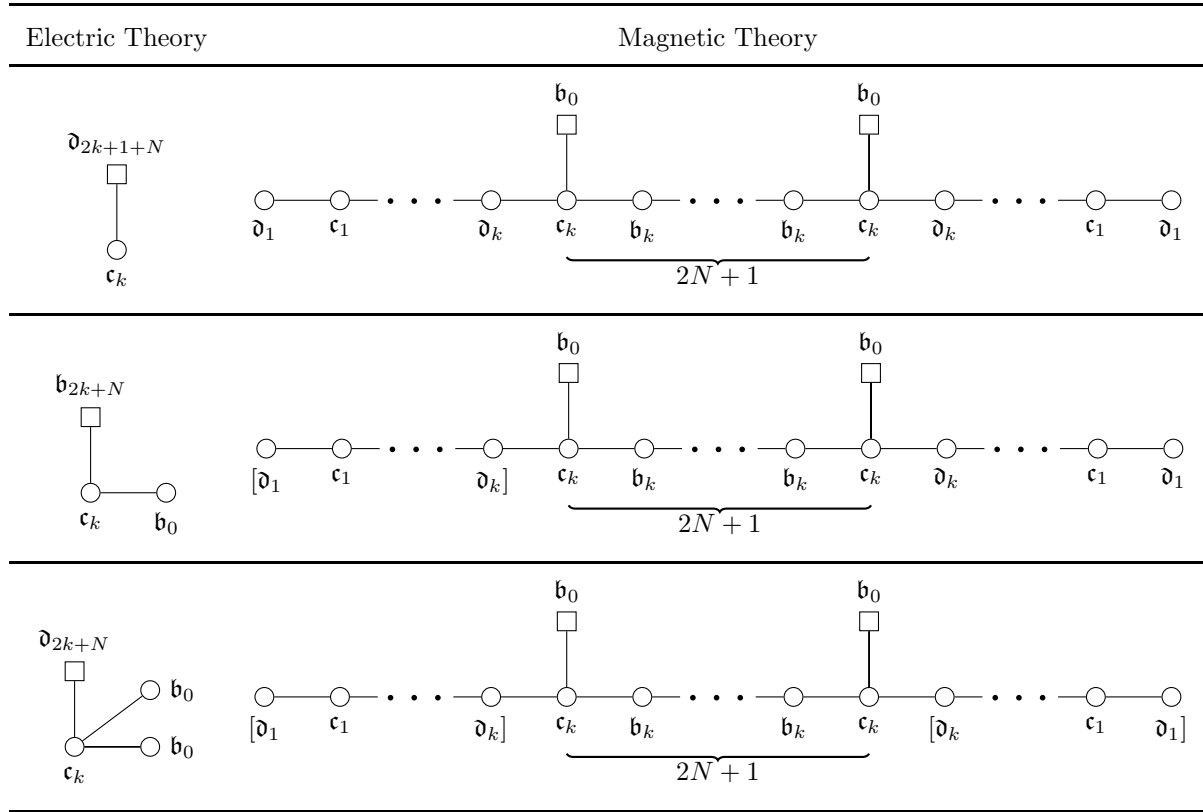


Table 2: The electric-magnetic pairs derived from brane systems for $\text{Sp}(k)$ SQCD with on or two \mathbb{Z}_2 gaugings. The gauging in the magnetic theory appears as a diagonal quotient on the magnetic lattice.

7 Outlook

This paper introduced several conjectures regarding the interpretation of discrete gaugings in brane systems involving D3-/D5-/NS5-branes with $O3$ orientifold planes and identities on the Coulomb branch from Higgsings within a special piece, supported using 3d mirror symmetry and Hilbert series computations.

It is also interesting to consider the fate of the Coulomb branch identity in Section 4.1 under 3d mirror symmetry. It appears that these identities lead to a map on the Higgs branch of a maximal BC -chain that decreases the rank of each node of B -type. Calculations show that this map keeps the Higgs branch invariant, despite manifest incomplete Higgsing. Similarly, calculations show that the diagonal \mathbb{Z}_2 gauging of a maximal DC -chain does not change the Higgs branch, which agrees with intuition from its electric counterpart – it would be useful to prove these statements.

It is also unclear as to why the Higgsing in Section 4.1 requires *all* $\frac{1}{2}$ D3-branes created under the splitting of a D5-brane to be removed. Removing only *some* of the red branes in Figure 9b leads to a brane system whose corresponding quiver theory cannot be read using current techniques.

It is possible to conjecture rules for framed orthosymplectic subtraction and perform rudimentary examples in the presence of the \mathbb{Z}_2 gaugings identified in this work. However, fundamental problems regarding the interpretation of D3-/D5-/NS5-brane systems with $O3$ orientifold planes circumscribe the set of identifiable transitions to those of type ADE with some exceptions [5]. Moreover, the brane system interpretation of the two cones in the Higgs branch of $\mathrm{Sp}(k)$ gauge theory with $2k$ flavours is also unclear [40, 41]. It would be helpful to settle these challenges in future work.

Given the various computational constraints imposed by orthosymplectic quivers, much of the topic remains unclear. In the first case, the identifications in (2.6) and (6.4) immediately give rise to the question of a string theory interpretation. A satisfactory answer may currently remain out of reach; it is unclear for instance whether this bears any relation to the introduction of spinor matter in [43].

Acknowledgments

We thank Rudolph Kalveks, Guhesh Kumaran, Hiraku Nakajima, Michael Finkelberg, Noppadol Mekareeya and William Harding for helpful discussions. The work of SB and AH is partially supported by STFC Consolidated Grants ST/T000791/1 and ST/X000575/1. SB is supported by the STFC DTP research studentship grant ST/Y509231/1.

A Evidence for Identities

This appendix contains evidence for the identities (4.4), (4.3) and (4.2) using the monopole formula to calculate unrefined Hilbert series. Identical unrefined Hilbert series are not sufficient for proving an equivalence of moduli spaces - at best they provide a strong indication of a match. In analogy to that given for the BC chain in Section 5, the proofs here proceed by recognising that the magnetic lattices and dressing factors are unchanged on either side of (4.4), (4.3) and (4.2). Hence it suffices to check that the conformal dimensions of the two quivers on each side of a given identity are equal, calculated explicitly below. First consider the identity given in (4.4), rewritten with its magnetic charges in Figure 15. The conformal dimension Δ_L of Figure 15a is given in (A.4), where $\Sigma_{\mathbf{c}_{k_1}}$ and $\Sigma_{\mathbf{c}_{k_3}}$ denote the vectormultiplet contributions from the $\mathrm{Sp}(k_1)$ and $\mathrm{Sp}(k_3)$ nodes and Σ_m collects terms of the form

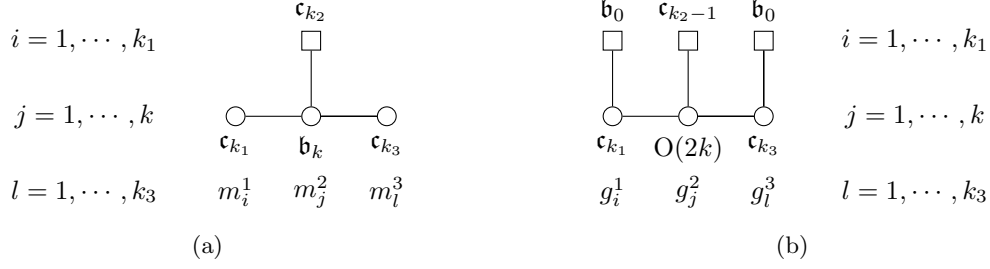


Figure 15: The identity given in (4.4) with magnetic charges assigned to each gauge node.

$|m^\alpha \pm m^\beta|$ ($\alpha, \beta = 1, 2, 3$) common to both Δ_L and Δ_R .

$$\Delta_L^{\text{Hyp}} = \frac{1}{2} \sum_{i,j} (|m_i^1 - m_j^2| + |m_i^1 + m_j^2|) + \frac{1}{2} \sum_i |m_i^1| + \frac{1}{2} \sum_{j,l} (|m_j^2 - m_l^3| + |m_j^2 + m_l^3|) \quad (\text{A.1})$$

$$+ \frac{1}{2} \sum_l |m_i^3| + k_2 \sum_j |m_j^2| \quad (\text{A.2})$$

$$\Delta_L^{\text{Vec}} = \Sigma_{c_{k_1}} + \Sigma_{c_{k_3}} - \sum_{a < b} (|m_a^2 + m_b^2| + |m_a^2 - m_b^2|) - \sum_j |m_j^2| \quad (\text{A.3})$$

$$\Delta_L = \Delta_L^{\text{Hyp}} + \Delta_L^{\text{Vec}} = \Sigma_m + \frac{1}{2} \sum_i |m_i^1| + \frac{1}{2} \sum_l |m_l^3| + (k_2 - 1) \sum_j |m_j^2| \quad (\text{A.4})$$

The conformal dimension Δ_R of Figure 15b is similarly computed in (A.8).

$$\Delta_R^{\text{Hyp}} = \frac{1}{2} \sum_{i,j} (|g_i^1 - g_j^2| + |g_i^1 + g_j^2|) + \frac{1}{2} \sum_{j,l} (|g_j^2 - g_l^3| + |g_j^2 + g_l^3|) + \frac{1}{2} \sum_i |g_i^1| \quad (\text{A.5})$$

$$+ \frac{1}{2} \sum_l |g_i^3| + (k_2 - 1) \sum_j |g_j^2| \quad (\text{A.6})$$

$$\Delta_R^{\text{Vec}} = \Sigma_{c_{k_1}} + \Sigma_{c_{k_3}} - \sum_{a < b} (|g_a^2 + g_b^2| + |g_a^2 - g_b^2|) \quad (\text{A.7})$$

$$\Delta_R = \Delta_R^{\text{Hyp}} + \Delta_R^{\text{Vec}} = \Sigma_g + \frac{1}{2} \sum_i |g_i^1| + \frac{1}{2} \sum_l |g_l^3| + (k_2 - 1) \sum_j |g_j^2| \quad (\text{A.8})$$

Since $m^{1,2,3}$ and $g^{1,2,3}$ are summed over the same lattice, the conformal dimension contributions of Figure 15a and Figure 15b are identical.

The identity given in (4.3), rewritten in Figure 16 alongside its magnetic charges, is similarly supported by a calculation using the unrefined Hilbert series. The conformal dimension for the quiver in Figure 16a is given in (A.12), in which

$$\Delta_L^{\text{Hyp}} = \frac{1}{2} \sum_{i,j} (|m_i^1 - m_j^2| + |m_i^1 + m_j^2|) + \sum_i |m_i^1| + \frac{1}{2} \sum_{j,l} (|m_j^2 - m_l^3| + |m_j^2 + m_l^3|) \quad (\text{A.9})$$

$$+ \sum_l |m_i^3| + k_2 \sum_j |m_j^2| \quad (\text{A.10})$$

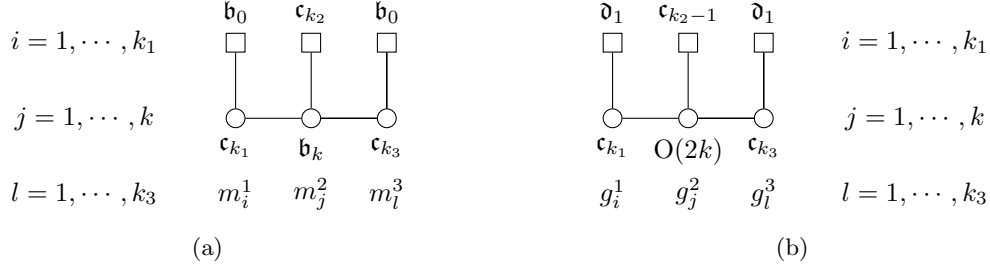


Figure 16: The identity given in (4.3) with magnetic charges assigned to each gauge node.

$$\Delta_L^{\text{Vec}} = \Sigma_{\mathbf{c}_{k_1}} + \Sigma_{\mathbf{c}_{k_3}} - \sum_{a < b} (|m_a^2 + m_b^2| + |m_a^2 - m_b^2|) - \sum_j |m_j^2| \quad (\text{A.11})$$

$$\Delta_L = \Delta_L^{\text{Hyp}} + \Delta_L^{\text{Vec}} = \Sigma_m + \sum_i |m_i^1| + \sum_l |m_l^3| + (k_2 - 1) \sum_j |m_j^2| \quad (\text{A.12})$$

The conformal dimension for the quiver in Figure 16b is given in (A.16)

$$\Delta_R^{\text{Hyp}} = \frac{1}{2} \sum_{i,j} (|g_i^1 - g_j^2| + |g_i^1 + g_j^2|) + \frac{1}{2} \sum_{j,l} (|g_j^2 - g_l^3| + |g_j^2 + g_l^3|) + \sum_i |g_i^1| \quad (\text{A.13})$$

$$+ \sum_l |g_l^3| + (k_2 - 1) \sum_j |g_j^2| \quad (\text{A.14})$$

$$\Delta_R^{\text{Vec}} = \Sigma_{\mathbf{c}_{k_1}} + \Sigma_{\mathbf{c}_{k_3}} - \sum_{a < b} (|g_a^2 + g_b^2| + |g_a^2 - g_b^2|) \quad (\text{A.15})$$

$$\Delta_R = \Delta_R^{\text{Hyp}} + \Delta_R^{\text{Vec}} = \Sigma_g + \sum_i |g_i^1| + \sum_l |g_l^3| + (k_2 - 1) \sum_j |g_j^2| \quad (\text{A.16})$$

It's clear by now that for general m, n in (4.2) the calculation proceeds in almost exactly the same way.

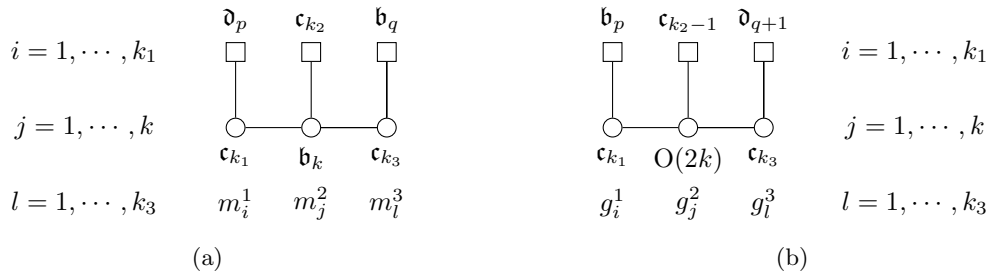


Figure 17: The identity given in (4.2) with magnetic charges assigned to each gauge node.

The conformal dimension for the quiver in Figure 17a, Δ_L , is given in (A.20).

$$\Delta_L^{\text{Hyp}} = \frac{1}{2} \sum_{i,j} (|m_i^1 - m_j^2| + |m_i^1 + m_j^2|) + p \sum_i |m_i^1| + \frac{1}{2} \sum_{j,q} (|m_j^2 - m_q^3| + |m_j^2 + m_q^3|) \quad (\text{A.17})$$

$$+ l \sum_q |m_q^3| + \frac{1}{2} \sum_q |m_q^3| + \frac{1}{2} \sum_q |m_q^3| + k_2 \sum_j |m_j^2| + \frac{1}{2} \sum_i |m_i^1| \quad (\text{A.18})$$

$$\Delta_L^{\text{Vec}} = \Sigma_{\mathbf{c}_{k_1}} + \Sigma_{\mathbf{c}_{k_3}} - \sum_{a < b} (|m_a^2 + m_b^2| + |m_a^2 - m_b^2|) - \sum_j |m_j^2| - \sum_j |m_j^2| \quad (\text{A.19})$$

$$\Delta_L = \Delta_L^{\text{Hyp}} + \Delta_L^{\text{Vec}} = \Sigma_m + (p + \frac{1}{2}) \sum_i |m_i^1| + (l + 1) \sum_q |m_q^3| + (k_2 - 1) \sum_j |m_j^2| \quad (\text{A.20})$$

The conformal dimension for the quiver in Figure 17b is similarly given in (A.24).

$$\Delta_R^{\text{Hyp}} = \frac{1}{2} \sum_{i,j} (|g_i^1 - g_j^2| + |g_i^1 + g_j^2|) + \frac{1}{2} \sum_{j,q} (|g_j^2 - g_q^3| + |g_j^2 + g_q^3|) + p \sum_i |g_i^1| \quad (\text{A.21})$$

$$+ (l + 1) \sum_q |g_q^3| + (k_2 - 1) \sum_j |g_j^2| + \frac{1}{2} \sum_i |g_i^1| \quad (\text{A.22})$$

$$\Delta_R^{\text{Vec}} = \Sigma_{\mathbf{c}_{k_1}} + \Sigma_{\mathbf{c}_{k_3}} - \sum_{a < b} (|g_a^2 + g_b^2| + |g_a^2 - g_b^2|) \quad (\text{A.23})$$

$$\Delta_R = \Delta_R^{\text{Hyp}} + \Delta_R^{\text{Vec}} = \Sigma_g + (p + \frac{1}{2}) \sum_i |g_i^1| + (l + 1) \sum_q |g_q^3| + (k_2 - 1) \sum_j |g_j^2| \quad (\text{A.24})$$

Again, since the m and g magnetic charges are summed over the same lattice, the two conformal dimensions contribute identically to their respective sums.

B Hilbert Series for BC Chains

This appendix contains the full unrefined Hilbert series for several of the BC -chain quivers $\mathcal{Q}_{B.1}$.

$$(B.1)$$

k	N	Hilbert Series	PL
1	1	$\frac{1+3t^2+11t^4+10t^6+11t^8+3t^{10}+t^{12}}{(1-t^4)^3(1-t^2)^3}$	$6t^2 + 8t^4 - 15t^6 - 4t^8 + \dots$
	2	$\frac{1+10t^2+55t^4+150t^6+288t^8+336t^{10}+288t^{12}+150t^{14}+55t^{16}+10t^{18}+t^{20}}{(1-t^4)^5(1-t^2)^5}$	$15t^2 + 5t^4 - 70t^6 + 273t^8 + \dots$
	3	$\frac{1+21t^2+189t^4+931t^6+3003t^8+6615t^{10}+10567t^{12}+12258t^{14}+\dots+t^{28}}{(1-t^4)^7(1-t^2)^7}$	$28t^2 - 35t^4 + 42t^6 + 336t^8 + \dots$
2	1	$\frac{1+6t^4+6t^6+26t^8+15t^{10}+76t^{12}+30t^{14}+107t^{16}+50t^{18}+\dots+t^{36}}{(1-t^8)^3(1-t^4)^3(1-t^2)^6}$	$6t^2 + 9t^4 + 6t^6 + 8t^8 - 21t^{10} - 31t^{12} + 47t^{16}$

Table 3: Unrefined Hilbert series for the Coulomb branches of several examples of the BC -chain quiver (B.1) labelled by (N, k) .

References

- [1] S. Cabrera and A. Hanany, *Quiver Subtractions*, *JHEP* **09** (2018) 008, [[1803.11205](#)].
- [2] K. Gledhill and A. Hanany, *Coulomb branch global symmetry and quiver addition*, *JHEP* **12** (2021) 127, [[2109.07237](#)].
- [3] A. Bourget, M. Sperling and Z. Zhong, *Decay and Fission of Magnetic Quivers*, [2312.05304](#).
- [4] S. Cabrera and A. Hanany, *Branes and the Kraft-Procesi Transition*, *JHEP* **11** (2016) 175, [[1609.07798](#)].
- [5] S. Cabrera and A. Hanany, *Branes and the Kraft-Procesi transition: classical case*, *JHEP* **04** (2018) 127, [[1711.02378](#)].
- [6] C. Hwang, S. Pasquetti and M. Sacchi, *Rethinking mirror symmetry as a local duality on fields*, *Phys. Rev. D* **106** (2022) 105014, [[2110.11362](#)].
- [7] R. Comi, C. Hwang, F. Marino, S. Pasquetti and M. Sacchi, *The $SL(2, \mathbb{Z})$ dualization algorithm at work*, *JHEP* **06** (2023) 119, [[2212.10571](#)].
- [8] S. Giacomelli, C. Hwang, F. Marino, S. Pasquetti and M. Sacchi, *Probing bad theories with the dualization algorithm. Part I*, *JHEP* **04** (2024) 008, [[2309.05326](#)].
- [9] S. Giacomelli, C. Hwang, F. Marino, S. Pasquetti and M. Sacchi, *Probing bad theories with the dualization algorithm. Part II.*, *JHEP* **07** (2024) 165, [[2401.14456](#)].

- [10] J. F. Grimminger, W. Harding and N. Mekareeya, *Wreathing, discrete gauging, and non-invertible symmetries*, *JHEP* **01** (2025) 124, [[2410.12906](#)].
- [11] S. Bennett, A. Hanany, G. Kumaran, C. Li, D. Liu and M. Sperling, *Quiver Subtraction on the Higgs Branch*, [2409.16356](#).
- [12] S. Bennett, A. Hanany and G. Kumaran, *Orthosymplectic quotient quiver subtraction*, *JHEP* **12** (2024) 063, [[2409.15419](#)].
- [13] A. Beauville, *Symplectic singularities*, *Inventiones mathematicae* **139** (2000) 541–549.
- [14] A. Bourget, S. Cabrera, J. F. Grimminger, A. Hanany, M. Sperling, A. Zajac et al., *The Higgs mechanism — Hasse diagrams for symplectic singularities*, *JHEP* **01** (2020) 157, [[1908.04245](#)].
- [15] A. Bourget, J. F. Grimminger, A. Hanany and Z. Zhong, *The Hasse diagram of the moduli space of instantons*, *JHEP* **08** (2022) 283, [[2202.01218](#)].
- [16] A. Bourget and J. F. Grimminger, *Fibrations and hasse diagrams for 6d SCFTs*, *Journal of High Energy Physics* **2022** (dec, 2022) .
- [17] J. F. Grimminger and A. Hanany, *Hasse diagrams for 3d $\mathcal{N} = 4$ quiver gauge theories — Inversion and the full moduli space*, *JHEP* **09** (2020) 159, [[2004.01675](#)].
- [18] V. Borokhov, A. Kapustin and X.-k. Wu, *Topological disorder operators in three-dimensional conformal field theory*, *JHEP* **11** (2002) 049, [[hep-th/0206054](#)].
- [19] V. Borokhov, A. Kapustin and X.-k. Wu, *Monopole operators and mirror symmetry in three-dimensions*, *JHEP* **12** (2002) 044, [[hep-th/0207074](#)].
- [20] A. Hanany and E. Witten, *Type IIB superstrings, BPS monopoles, and three-dimensional gauge dynamics*, *Nucl. Phys. B* **492** (1997) 152–190, [[hep-th/9611230](#)].
- [21] A. Hanany and A. Zaffaroni, *Issues on orientifolds: On the brane construction of gauge theories with $SO(2n)$ global symmetry*, *JHEP* **07** (1999) 009, [[hep-th/9903242](#)].
- [22] A. Hanany and J. Troost, *Orientifold planes, affine algebras and magnetic monopoles*, *Journal of High Energy Physics* **2001** (Aug., 2001) 021–021.
- [23] B. Feng and A. Hanany, *Mirror symmetry by $o\bar{3}$ -planes*, *Journal of High Energy Physics* **2000** (Nov., 2000) 033–033.
- [24] D. Juteau, P. Levy and E. Sommers, *Minimal special degenerations and duality*, *arXiv e-prints* (Sept., 2023) arXiv:2310.00521, [[2310.00521](#)].
- [25] B. Fu, D. Juteau, P. Levy and E. Sommers, *Generic singularities of nilpotent orbit closures*, *arXiv e-prints* (Feb., 2015) arXiv:1502.05770, [[1502.05770](#)].
- [26] E. Sommers, *Lusztig’s canonical quotient and generalized duality*, *Journal of Algebra* **243** (2001) 790–812.
- [27] N. Marcus and A. Sagnotti, *Tree-level constraints on gauge groups for type i superstrings*, *Physics Letters B* **119** (1982) 97–99.
- [28] S. Cabrera, A. Hanany and Z. Zhong, *Nilpotent orbits and the Coulomb branch of $T^\sigma(G)$ theories: special orthogonal vs orthogonal gauge group factors*, *JHEP* **11** (2017) 079, [[1707.06941](#)].
- [29] S. Cabrera, A. Hanany and R. Kalveks, *Quiver Theories and Formulae for Slodowy Slices of Classical Algebras*, *Nucl. Phys. B* **939** (2019) 308–357, [[1807.02521](#)].
- [30] A. Bourget and A. Pini, *Non-Connected Gauge Groups and the Plethystic Program*, *JHEP* **10** (2017) 033, [[1706.03781](#)].

- [31] A. Hanany and R. Kalveks, *Quiver Theories for Moduli Spaces of Classical Group Nilpotent Orbits*, *JHEP* **06** (2016) 130, [[1601.04020](#)].
- [32] E. Witten, *An $SU(2)$ Anomaly*, *Physics Letters B* **117** (1982) 324–328.
- [33] P. N. Achar, *An order-reversing duality map for conjugacy classes in Lusztig’s canonical quotient*, *Transformation Groups* **8** (2003) 107–145.
- [34] A. Bourget and J. F. Grimminger, *Fibrations and Hasse diagrams for 6d SCFTs*, *JHEP* **12** (2022) 159, [[2209.15016](#)].
- [35] A. Hanany and G. Zafrir, *Discrete Gauging in Six Dimensions*, *JHEP* **07** (2018) 168, [[1804.08857](#)].
- [36] S. Cremonesi, A. Hanany and A. Zaffaroni, *Monopole operators and Hilbert series of Coulomb branches of 3d $\mathcal{N} = 4$ gauge theories*, *JHEP* **01** (2014) 005, [[1309.2657](#)].
- [37] A. Hanany and M. Sperling, *Algebraic properties of the monopole formula*, *JHEP* **02** (2017) 023, [[1611.07030](#)].
- [38] D. Juteau, P. Levy and E. Sommers, *Minimal special degenerations and duality*, *arXiv preprint arXiv:2310.00521* (2023) .
- [39] B. Fu, D. Juteau, P. Levy and E. Sommers, *Local geometry of special pieces of nilpotent orbits*, *arXiv e-prints* (Aug., 2023) arXiv:2308.07398, [[2308.07398](#)].
- [40] G. Ferlito and A. Hanany, *A tale of two cones: the Higgs Branch of $Sp(n)$ theories with $2n$ flavours*, [1609.06724](#).
- [41] A. Bourget, J. F. Grimminger, A. Hanany, R. Kalveks, M. Sperling and Z. Zhong, *A tale of N cones*, *JHEP* **09** (2023) 073, [[2303.16939](#)].
- [42] A. Kapustin and M. J. Strassler, *On mirror symmetry in three dimensional abelian gauge theories*, *Journal of High Energy Physics* **1999** (Apr., 1999) 021–021.
- [43] G. Zafrir, *Brane webs and $O5$ -planes*, *JHEP* **03** (2016) 109, [[1512.08114](#)].